Research Article | Vol. 28, No. 16 / 3 August 2020 / Optics Express 23114
Optics EXPRESS

Laser emission at 4.5 THz from $^{15}NH_3$ and a mid-infrared quantum-cascade laser as a pump source

MARTIN WIENOLD,[1,*] ALSU ZUBAIROVA,[1] AND HEINZ-WILHELM HÜBERS[1,2]

[1]German Aerospace Center (DLR), Institute of Optical Sensor Systems, Rutherfordstr. 2, 12489 Berlin, Germany
[2]Humboldt-Universität zu Berlin, Department of Physics, Newtonstr. 15, 12489 Berlin, Germany
[*]martin.wienold@dlr.de

Abstract: We present an optically pumped terahertz gas laser, which is based on a mid-infrared quantum-cascade laser as a pump source, a transversely pumped standing wave resonator, and $^{15}NH_3$ as a gain medium. We observe several laser lines around 4.5 THz, corresponding to rotational transitions in the ν_2 band of ammonia. So far, these are the highest frequencies obtained from a QCL-pumped THz gas laser. The involved molecular transitions are unambiguously identified by high-resolution spectroscopy.

1. Introduction

Being highly brilliant continuous wave emitters, optically pumped terahertz (THz) gas lasers have been longstanding sources for a variety of applications from THz imaging, spectroscopy to detector characterization and calibration [1–3]. THz gas lasers have been even used in space and airborne applications such as the 2.5-THz local oscillator for the microwave limb sounder on NASA's Aura satellite [4]. However, the usually employed CO_2 pump lasers are rather bulky, and although there exist a large number of CO_2 laser lines in the mid-infrared between 9 and 11 µm, the frequency of these lines can only be tuned by a few MHz. Pumping molecular transitions requires therefore a close-by ro-vibrational resonance of the gain species. Since the number of transitions increases for larger molecules – and therefore the probability to match a CO_2 laser line – examples for prominent THz gas laser species are methanol (CH_3OH), difluoromethane (CH_2F_2), and formic acid (HCOOH) [5]. Although transition line strengths substantially increase for lighter molecules such as ammonia, the lack of coinciding pump transitions does not allow for the use of regular CO_2 lasers. Obtaining lasing from molecules such as ammonia requires therefore special means, such as CO_2 lasers emitting in a sequence band, special isotope compositions, or an additional electric field in the kV/cm range to shift resonances by the Stark effect [6–9]. In contrast to pumping with a CO_2 laser, the frequency of mid-infrared QCLs can be continuously tuned over a range of typically several hundred GHz. Thanks to the maturity of mid-infrared QCL technology, continuous-wave devices with customer-specified emission range are nowadays commercially available. Although their output power is at the best a few hundred mW and therefore several orders of magnitude smaller than that of CO_2 lasers, this drawback is mitigated by the possibility of resonant pumping and the strong dipole transitions of molecules such as ammonia. With respect to the spectral brightness and output power of molecular lasers, the only mature alternative are currently QCLs in the THz range [10,11]. However, THz QCLs require cryogenic cooling, while molecular lasers have the advantage to operate under ambient

#395832 https://doi.org/10.1364/OE.395832
Journal © 2020 Received 22 Apr 2020; revised 22 Jun 2020; accepted 30 Jun 2020; published 20 Jul 2020

Optics EXPRESS

conditions. In view of the power consumption and weight of cryocoolers, this is a substantial benefit for instrument development in particular for space applications.

The development of QCL pumped molecular lasers started in 2016 with the work of Pagies *et al.* [12]. However, all previous reports showed lasing only below 1 THz [12–15], a range for which more convenient electronic multiplier sources are already available. Here, we report QCL-pumped lasing for rotational transitions of $^{15}NH_3$ at much higher frequencies around 4.5 THz, based on an alternative resonator approach and by exploiting the molecular symmetry to avoid low-frequency laser transitions. A potentially important application of a QCL-pumped molecular laser is heterodyne detection of atomic oxygen, which has its ground state transition at 4.7 THz [16,17].

2. Experimental configuration

The transversely pumped standing-wave resonator is based on a 80-cm long circular copper waveguide with a diameter of 20 mm, two spherical resonator mirrors with 1 m radius, and an outcoupling mirror. Figure 1(a) depicts a photography of the setup and Fig. 1(b) a schematics of the resonator. The pump radiation is coupled under oblique incidence via a ZnSe Brewster window into the copper waveguide. The position of one of the resonator mirrors can be tuned by a piezo-motorized actuator in order to match the Fabry-Pérot resonance condition. THz laser emission is extracted via a movable outcoupling mirror and a high-density polyethylene (HDPE) window. This configuration has the advantage of being robust against misalignment of the pump source as well as being flexible with respect to the outcoupling which can be adjusted by the moveable outcoupling mirror. By this means also weak laser lines can be operated. The price to pay is a non-ideal overlap with the fundamental cavity mode. Due to the "off-axis" pumping scheme no optical isolator is required to protect the pump source from optical feedback.

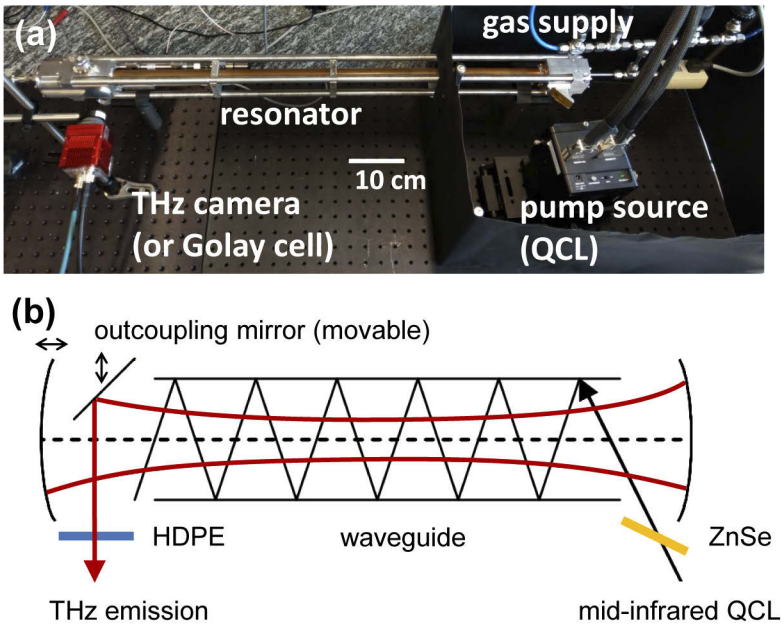

Fig. 1. (a) Photography of the molecular gas laser setup. (b) Schematics of the transversely pumped resonator.

We used a commercial distributed-feedback mid-infrared QCL as a pump source (Thorlabs). The laser provides single-mode emission with up to 230 mW at 15°C heat sink temperature,

Optics EXPRESS

decreasing to about 150 mW (max) at 30°C. The frequency of the source can be tuned by varying the heat sink temperature and the driving current and covers a continuous frequency range of 190 GHz between 9.23-9.29 µm. For precise frequency calibration, we performed absorption spectroscopy with CH_3OH, which exhibits well known transitions in the whole range accessible with the pump QCL. We obtained frequency tuning parameters of −0.38 GHz/mA and −2.52 GHz/K. Since the power increases above threshold with about 0.6 W/A, pump-power dependent measurements become possible by varying the driving current and the heatsink temperature at the same time.

3. $^{15}NH_3$ as a gain medium

Figure 2(a) depitcs several strong rovibrational transitions of $^{15}NH_3$ which are covered by the QCL. For obtaining the spectrum, the QCL frequency was varied by slowly ramping up the driving current at a heat sink temperature of 25°C. The transmission of a 118-cm-long gas cell was recorded by integrating the image signal of a room temperature microbolometer camera (FLIR, Tau2). These transitions are identified as the saR(5,1) to saR(5,5) transition of $^{15}NH_3$ [18]. Figure 2(b) shows a simulated spectrum based on the ExoMol database [19], which unambiguously confirms the identified transitions by the spectral fingerprint.

Figure 3 depicts an overview of the involved energy levels and transitions. For example, saR(5,0) represents the transition between $v = 0$, $J_K = 5_0$(s) and $v_2 = 1$, $J_K = 6_0$(a) with quantum numbers J and K and symmetry s (symmetric) or a (antisymmetric). In principle, several laser transitions are possible. Beside the direct rotational transitions in the v_2 band [e.g. $J_K = 6_0$(a)→ 5_0(s)], lasing from the inversion transitions 6_K(a)→ 6_K(s) should be possible as well for K>0. [9,12] For $K = 0$, lasing of pure inversion transitions is prohibited by symmetry. In addition to that, refilling transitions in the $v = 0$ band might contribute to lasing for large pump powers.

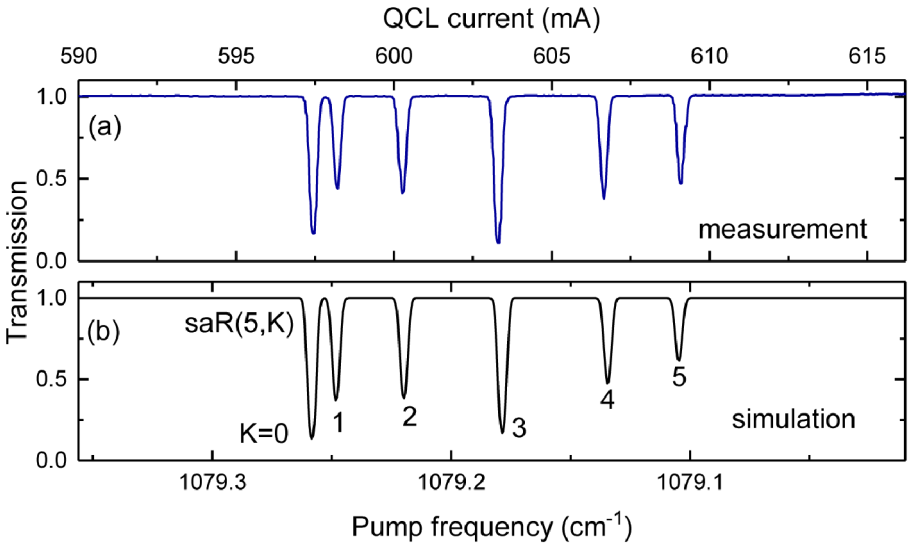

Fig. 2. (a) Measured absorption spectrum and (b) simulated unsaturated absorption of $^{15}NH_3$ for the saR(5,0)· · · saR(5,5) transitions for a 118 cm long gas cell at 1 Pa pressure.

Optics EXPRESS

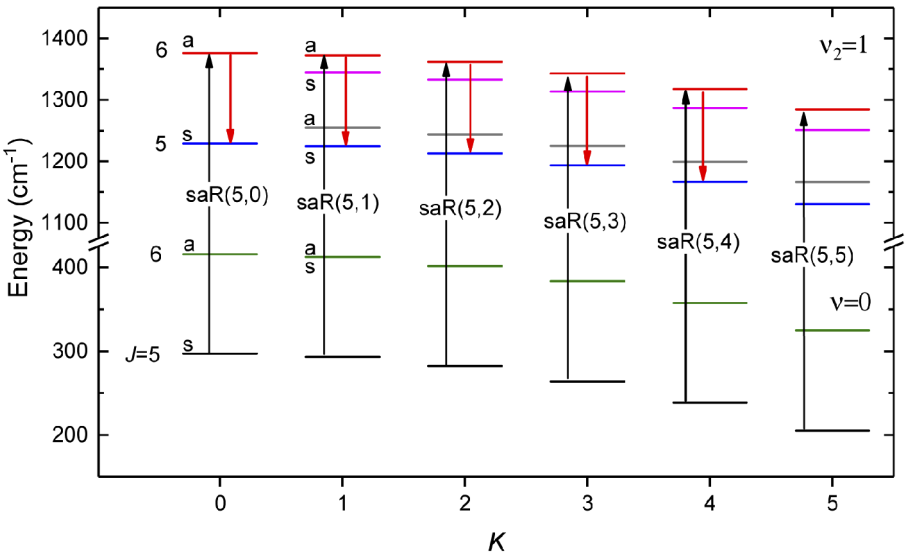

Fig. 3. Involved energy levels, pump transitions (black arrows) and observed lasing transitions (red arrows) of $^{15}NH_3$ for the covered pump range.

4. Laser characteristics

Figure 4(a) depicts the THz emission signal as a function of the resonator length for the different pump transitions. The scans reveal a periodic pattern, which represents the Fabry-Pérot condition, i.e. the peak-to-peak period corresponds to $\lambda/2$. Peaks of different height correspond to different transversal modes, which will be discussed in more detail later. Laser emission with decreasing intensity is observed for pump transitions up to $K = 4$, while no emission is observed for $K = 5$ [Fig. 4(b)]. The intensity decrease from $K = 0$ to $K = 1$ is explained by the reduced number of states for $K = 0$ due to symmetry resulting in the absence of parasitic relaxation channels. The intensity decrease toward higher K numbers and the absence of lasing for $K = 5$ is not explained by the variation of pump line strength. An additional K-number related relaxation channel or bottleneck might play a role here. Depending on the air humidity, the intensity measurements for $K>1$ become also affected by the presence of water absorption lines between 149 and 154 cm^{-1}. For our typical lab conditions we estimate a maximum of 25% attenuation for the $K = 4$ transition at 151.18 cm^{-1} and 75% for the unobserved $K = 5$ transitions at 153.51 cm^{-1}.

We found a dip in the line center for all the laser peaks, an effect known as transferred Lamb dip [20], which occurs in the presence of counter propagating pump waves and becomes especially pronounced for transverse pumping geometries. The depth of the dip depend on several parameters, such as the pump saturation. The asymmetry of the dip as seen in Fig. 4(c) is caused by a marginal detuning of the pump laser from the molecular resonance. In principle, laser stabilization can be achieved by locking the emission frequency to the Lamb dip.

In contrast to Refs. [12,15], we did not observe lasing from pure inversion transitions as well as from refilling transitions. This was confirmed by performing longer cavity scans including the longest potential transition wavelength, which, in our case, would be 358 µm for the $J_K = 6_1(a) \rightarrow 6_1(s)$ inversion transition. In case of the saR(5,0) pump transition, pure inversion transitions do not exist due to symmetry. For larger K-numbers the absence of such laser lines might be a consequence of the resonator layout and the transverse pumping scheme favoring lasing transitions which are higher in frequency. Refilling transitions might not be observed for the same reason as well as due to a lack of pump power. A list of the identified laser transitions

Optics EXPRESS

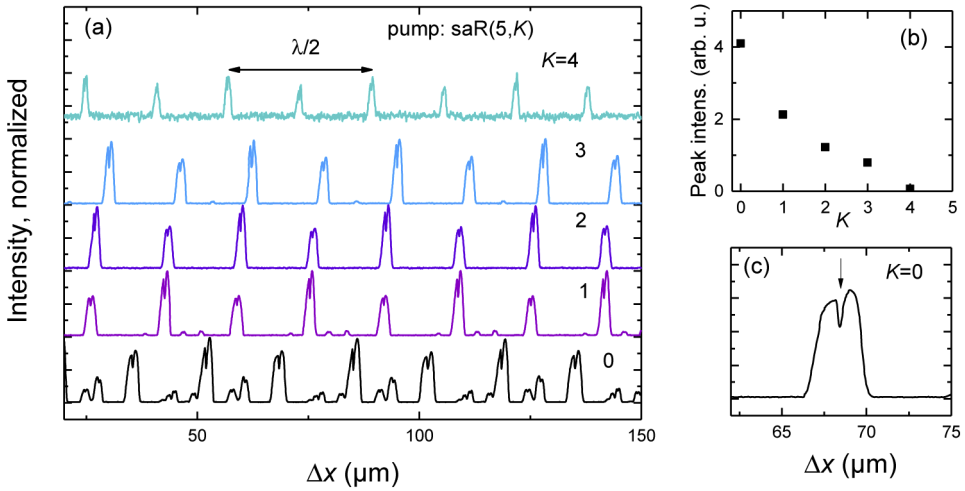

Fig. 4. (a) Output intensity vs. resonator length variation (Δx) for the saR(5,0)$\cdots$saR(5,4) pump transitions, measured unfocused with a Golay cell detector and a HDPE plate as mid-infrared blocking filter, step size: 40 nm. The peaks represent THz laser emission. The periodicity corresponds to the Fabry-Pérot laser condition, and allows for determining the emission wavelength. (b) Comparison of the THz peak intensity for the different pump transitions. (c) Magnified emission peak with distinct transferred Lamb dip (arrow).

is given in Table 1. The increase of frequency with increasing K-number is consistent with theory. Absolute values deviate but are still within the 1% uncertainty of the resonator length scan measurements.Fig. 5 depicts the THz laser intensity as a function of pressure for the most intense line [6_0(a) $\rightarrow$ 5_0(s)] and three different pump power values. The laser intensity maximum is found for 1 Pa and 210 mW pump power, corresponding to 30 μW incident power on the Golay cell. Toward lower pressure the output power decreases due to the reducing number of molecules contributing to gain. Toward higher pressure the power decrease is due to non-radiative collisional relaxations of molecules. The maximum power conversion efficiency is 1.4×10^{-4}. Although this is a fairly low number compared to the general Manley-Rowe (MR) limit given by $\nu_{\mathrm{THz}}/\nu_{\mathrm{pump}} = 0.13$, the MR efficiency of 1×10^{-3}, i.e. power efficiency divided by the MR limit, is consistent to what was obtained for the same cavity by pumping with a CO_2 laser. Higher-efficiency molecular gas lasers reach typically 10% of the MR limit [4], with record values of 15 – 29% [21–23] and a theoretical maximum of 50% for these lasers. Therefore, output powers in the mW range for an efficiency-optimized resonator design appear realistic.

Table 1. List of observed THz laser transitions,[a] pump frequencies (ν_{pump}), and laser frequencies (ν_{las}) according to Ref. [19]. Experimental values (ν_{exp}) are determined from the cavity scan with an uncertainty of ca. 1%.

K	Laser transition	ν_{pump} cm^{-1}	ν_{las} THz	ν_{las} cm^{-1}	ν_{exp} cm^{-1}
0	6_0(a) $\rightarrow$ 5_0(s)	1079.26	4.417	147.34	148.6
1	6_1(a) $\rightarrow$ 5_1(s)	1079.25	4.424	147.57	149.1
2	6_2(a) $\rightarrow$ 5_2(s)	1079.22	4.445	148.26	149.6
3	6_3(a) $\rightarrow$ 5_3(s)	1079.18	4.480	149.45	152.1
4	6_4(a) $\rightarrow$ 5_4(s)	1079.13	4.532	151.18	152.8

[a]All are direct rotational transitions in the ν_2 band.

Optics EXPRESS

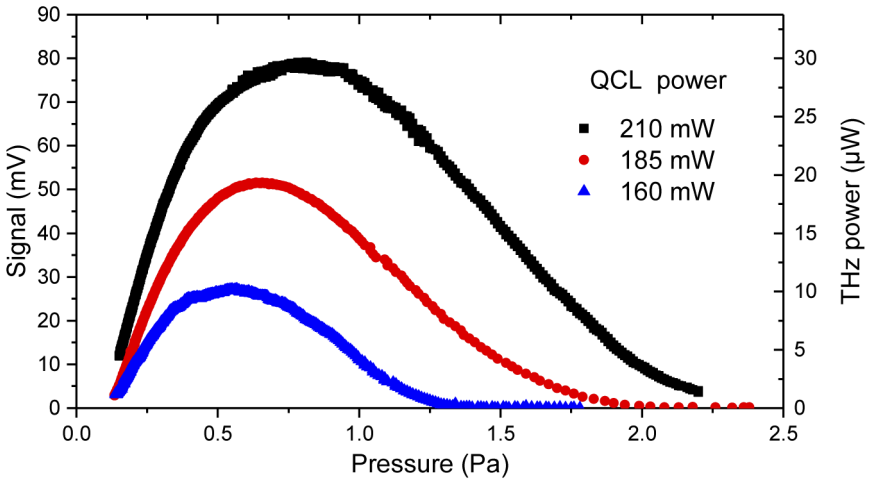

Fig. 5. THz laser intensity as a function of pressure for the saR(5,0) pump transition as measured with a Golay cell (2.5 mm aperture). The peak signal corresponds to an incident power of 30μW (8μW) on the Golay cell with (without) HDPE lens (f = 28 mm focal length).

Due to the pumping scheme, various transversal laser modes can be excited. These can be observed as beam profile variations by replacing the single-pixel Golay cell with a microbolometer camera (FLIR, tau2) equipped with an HDPE lens (f = 28 mm), which acts also as mid-infrared

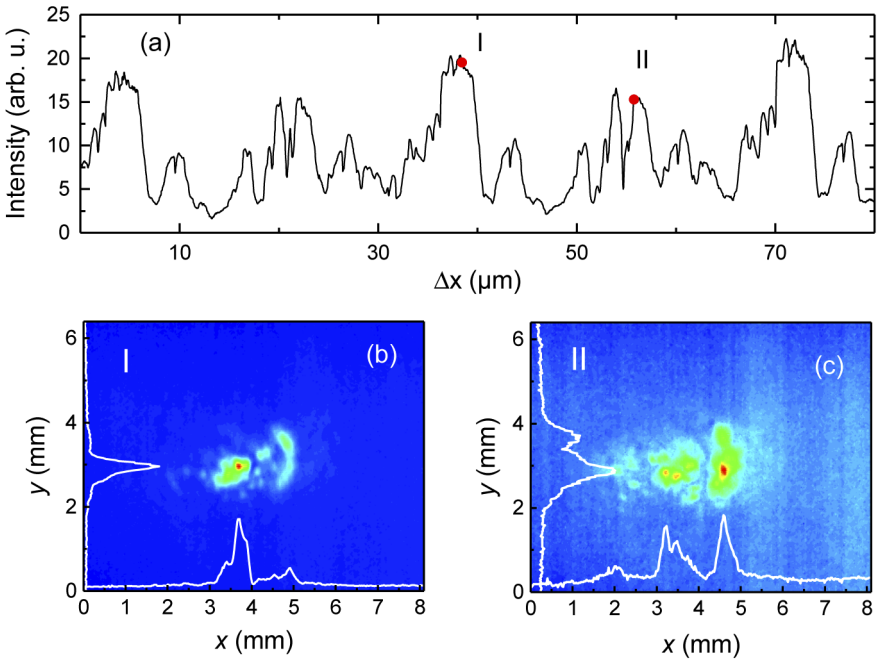

Fig. 6. (a) Integrated camera signal vs. resonator length variation. (b),(c) Intensity profiles for positions I and II in (a), indicating the presence of different lateral modes. x, y refer to the horizontal and vertical direction of the camera sensor, respectively. The baseline offset is caused by the thermal background.

Optics EXPRESS

blocking filter. The measurement is then similar to the resonator length scan as shown in Fig. 4, although in case of the microbolometer camera no chopper and lock-in amplifier are required. For the saR(5,0) pump transition, the integrated camera signal is shown in Fig. 6(a). Similar to Fig. 4(a), various peaks with a periodicity of 32 µm are observed. The larger number of peaks in Fig. 6(a) is a consequence of the larger sensitive area of the microbolometer array. For that reason, the camera is sensitive to a larger number of transversal (i.e. spatial) laser modes than the configuration with Golay cell. As exemplary shown in the Figs. 6(a) and (b), each of the peaks correspond to a different beam profile, reflecting the various transversal modes. For a cylindrical hollow core cavity, as a reasonable approximation of our laser resonator, cavity modes of different transversal order are separated in frequency by up to 20 MHz, while the longitudinal mode spacing is 190 MHz. From an application point of view, spatial filters might have to be applied in case a more Gaussian-like beam profile is required.

5. Conclusions

We presented a molecular gas laser based on $^{15}NH_3$ and a mid-infrared quantum-cascade laser as a pump source. We were able to obtain lasing from several rotational transitions around 4.5 THz, which this is so far the highest frequency obtained from a QCL-pumped THz gas laser. The output power is up to 30 µW. Although this would be already sufficient for pumping a hot electron bolometric mixer in a heterodyne receiver, we expect further substantial increase of output power for efficiency-optimized resonator designs. The two main advantages of a QCL-pumped THz gas laser as compared to a THz QCL are operation at ambient temperature and a well defined emission frequency. Therefore cryogenic cooling and active frequency stabilization are not necessary. This makes such a system very attractive as local oscillator in a THz heterodyne spectrometer provided that continuous frequency tuning is not required.

Disclosures

The authors declare no conflicts of interest.

References

1. D. M. Mittleman, "Twenty years of terahertz imaging," Opt. Express **26**(8), 9417–9431 (2018).
2. G. A. Blake, K. B. Laughlin, R. C. Cohen, K. L. Busarow, D. Gwo, C. A. Schmuttenmaer, D. W. Steyert, and R. J. Saykally, "The Berkeley tunable far infrared laser spectrometers," Rev. Sci. Instrum. **62**(7), 1701–1716 (1991).
3. A. Steiger, M. Kehrt, C. Monte, and R. Müller, "Traceable terahertz power measurement from 1 THz to 5 THz," Opt. Express **21**(12), 14466–14473 (2013).
4. E. R. Mueller, R. Henschke, J. William E. Robotham, L. A. Newman, L. M. Laughman, R. A. Hart, J. Kennedy, and H. M. Pickett, "Terahertz local oscillator for the microwave limb sounder on the Aura satellite," Appl. Opt. **46**(22), 4907–4915 (2007).
5. K. J. Button, M. Inguscio, and F. Struma, eds., *Reviews of infrared and millimeter waves*, vol. 2 (Plenum Press, New York, 1984).
6. E. J. Danielewicz and C. O. Weiss, "Far infrared laser emission from $^{15}NH_3$ optically pumped by a cw sequence band CO_2 laser," IEEE J. Quantum Electron. **14**(4), 222–223 (1978).
7. M. Redon, C. Gastaud, and M. Fourrier, "New cw far-infrared lasing in $^{14}NH_3$ using stark tuning," IEEE J. Quantum Electron. **15**(6), 412–414 (1979).
8. C. Gastaud, A. Sentz, M. Redon, and M. Fourrier, "Continuous-wave stark far-infrared lasing lines in $^{15}NH_3$ optically pumped by a CO_2 or N_2O laser," Opt. Lett. **6**(9), 449–451 (1981).
9. E. M. Frank, C. O. Weiss, K. Siemsen, M. Grinda, and G. D. Willenberg, "Predictions of far-infrared laser lines from $^{14}NH_3$ and $^{15}NH_3$," Opt. Lett. **7**(3), 96–98 (1982).
10. B. S. Williams, "Terahertz quantum-cascade lasers," Nat. Photonics **1**(9), 517–525 (2007).
11. H.-W. Hübers, H. Richter, and M. Wienold, "High-resolution terahertz spectroscopy with quantum-cascade lasers," J. Appl. Phys. **125**(15), 151401 (2019).
12. A. Pagies, G. Ducournau, and J.-F. Lampin, "Low-threshold terahertz molecular laser optically pumped by a quantum cascade laser," APL Photonics **1**(3), 031302 (2016).
13. A. Pagies, G. Ducournau, and J. Lampin, "Progress in continuous wave THz molecular laser optically pumped by a quantum cascade laser," in *2017 42nd International Conference on Infrared, Millimeter, and Terahertz Waves (IRMMW-THz)*, (2017), pp. 1–2.

Optics EXPRESS

14. M. Mičica, S. Eliet, M. Vanwolleghem, R. Motiyenko, A. Pienkina, L. Margulès, K. Postava, J. Pištora, and J.-F. Lampin, "High-resolution THz gain measurements in optically pumped ammonia," Opt. Express **26**(16), 21242–21248 (2018).
15. P. Chevalier, A. Amirzhan, F. Wang, M. Piccardo, S. G. Johnson, F. Capasso, and H. O. Everitt, "Widely tunable compact terahertz gas lasers," Science **366**(6467), 856–860 (2019).
16. R. T. Boreiko and A. L. Betz, "Heterodyne spectroscopy of the 63 μm OI line in M42," Astrophys. J. **464**(1), L83–L86 (1996).
17. H. Richter, M. Wienold, L. Schrottke, K. Biermann, H. T. Grahn, and H.-W. Hübers, "4.7-THz local oscillator for the GREAT heterodyne spectrometer on SOFIA," IEEE Trans. Terahertz Sci. Technol. **5**(4), 539–545 (2015).
18. G. D. Lonardo, L. Fusina, A. Trombetti, and I. M. Mills, "The ν_2, $2\nu_2$, $3\nu_2$, ν_4, and $\nu_2 + \nu_4$ bands of $^{15}NH_3$," J. Mol. Spectrosc. **92**, 298–325 (1982).
19. S. N. Yurchenko, "A theoretical room-temperature line list for $^{15}NH_3$," J. Quant. Spectrosc. Radiat. Transfer **152**, 28–36 (2015).
20. F. S. M. Inguscio and A. Moretti, "IR-FIR transferred Lamb-dip spectroscopy in optically pumped molecular lasers," Opt. Commun. **30**(3), 355–360 (1979).
21. E. J. Danielewicz, T. A. Galantowicz, F. B. Foote, R. D. Reel, and D. T. Hodges, "High performance at new FIR wavelengths from optically pumped CH_2F_2," Opt. Lett. **4**(9), 280–282 (1979).
22. J.-F. Lampin, A. Pagies, G. Santarelli, J. Hesler, W. Hansel, R. Holzwarth, and S. Barbieri, "Quantum cascade laser-pumped terahertz molecular lasers: frequency noise and phase-locking using a 1560 nm frequency comb," Opt. Express **28**(2), 2091–2106 (2020).
23. F. Wang, J. Lee, D. J. Phillips, S. G. Holliday, S.-L. Chua, J. Bravo-Abad, J. D. Joannopoulos, M. Soljačić, S. G. Johnson, and H. O. Everitt, "A high-efficiency regime for gas-phase terahertz lasers," Proc. Natl. Acad. Sci. **115**(26), 6614–6619 (2018).